Divergent responses of evergreen needle-leaf forests in Europe to the 2020 warm winter

Working Paper

Author(s):
Gharun, Mana; Shekhar, Ankit ⓘD; Hörtnagl, Lukas ⓘD; Krebs, Luana; Arriga, Nicola; Migliavacca, Mirco; Roland, Marilyn; Gielen, Bert; Montagnani, Leonardo; Tomelleri, Enrico; Šigut, Ladislav; Peichl, Matthias; Zhao, Peng; Schmidt, Marius; Grünwald, Thomas; Korkiakoski, Mika; Lohila, Annalea; Buchmann, Nina ⓘD

1 **Divergent responses of evergreen needle-leaf forests in Europe to the 2020 warm winter**
2
3 Mana Gharun[1], Ankit Shekhar[2], Lukas Hörtnagl[2], Luana Krebs[2], Nicola Arriga[3], Mirco
4 Migliavacca[3], Marilyn Roland[4], Bert Gielen[4], Leonardo Montagnani[5], Enrico Tomelleri[5],
5 Ladislav Šigut[6], Matthias Peichl[7], Peng Zhao[7], Marius Schmidt[8], Thomas Grünwald[9], Mika
6 Korkiakoski[10], Annalea Lohila[10], Nina Buchmann[2]
7
8 [1] Institute of Landscape Ecology, University of Münster, Germany
9 [2] Department of Environmental Systems Science, Institute of Agricultural Sciences, ETH
10 Zurich, Switzerland
11 [3] European Commission, Joint Research Centre (JRC), Ispra, Italy
12 [4] Plants and Ecosystems (PLECO), Department of Biology, University of Antwerp, 2610
13 Wilrijk, Belgium
14 [5] Free University of Bolzano, Faculty of Agricultural, Environmental and Food Sciences,
15 39100 Bolzano, Italy
16 [6] Global Change Research Institute CAS, Bělidla 986/4a, CZ-60300 Brno, Czech Republic,
17 ORCID: 0000-0003-1951-4100
18 [7] Department of Forest Ecology and Management, Swedish University of Agricultural
19 Sciences (SLU), SE-901 83 Umeå, Sweden
20 [8] Agrosphere (IBG-3), Institute of Bio- and Geosciences, Jülich Research Centre, 52425
21 Jülich, Germany
22 [9] Institute of Hydrology and Meteorology, Technical University of Dresden, Dresden,
23 Germany
24 [10] Finnish Meteorological Institute, Climate System Research, Helsinki Finland
25
26 Corresponding author: Mana Gharun (mana.gharun@uni-muenster.de)
27
28
29 **Abstract**
30 Relative to drought and heat waves, the effect of winter warming on forest CO_2 fluxes during
31 the dormant season has less been investigated, despite its relevance for net CO_2 uptake in colder
32 regions with higher carbon content in soils. Our objective was to test the effect of the
33 exceptionally warm winter in 2020 on the winter CO_2 budget of cold-adapted evergreen needle-
34 leaf forests across Europe, and identify the contribution of soil and air temperature to changes
35 in winter CO_2 fluxes in response to warming. Our hypothesis was that warming in winter leads
36 to higher emissions across colder sites due to increased ecosystem respiration. To test this
37 hypothesis, we used 98 site-year eddy covariance measurements across 14 evergreen needle-
38 leaf forests (ENFs) distributed from north to south of Europe (from Sweden to Italy). We used
39 a data-driven approach to quantify the effect of air and soil temperature on changes in net
40 ecosystem productivity (NEP) during the warm winter of 2020. Our results showed that the
41 impact of warming was different across sites, as in the lower altitude and lower latitude sites
42 positive soil temperature anomalies were larger, while positive air temperature anomalies were
43 larger in the northern latitude and high-altitude sites. Warming in winter led to a divergent

44   response across the sites. Out of 14 sites only in 3 sites net ecosystem productivity declined in

45   winter significantly in response to warming. In addition, we observed that in the colder sites

46   daytime NEP (that is dominated by photosynthesis) declined with warming of the air in winter,

47   whereas in the warmer sites daytime NEP increased with warming of the soil. While warming

48   increases ecosystem respiration, it might not trigger productivity in winter if the soil within the

49   rooting zone remains frozen. Forests within the same plant functional type category can exhibit

50   differing reactions to winter warming and to predict their responses accurately it is crucial to

51   account for variations in local climate, physiology, and structure simultaneously.

52
53   **Keywords:** eddy covariance, respiration, productivity, long-term, extremes, carbon flux
54
55
56
57   **Introduction**

58   One of the largest sources of uncertainties in understanding how forests can mitigate climate

59   change is the variation of forest CO_2 fluxes in response to extreme climatic conditions. Forests

60   absorb a large part of anthropogenic CO_2 emissions (Friedlingstein et al. 2023), but extreme

61   climatic conditions compromise the capacity of forests for carbon sequestration (Shekhar et al.

62   2023). While a large body of research focuses on extreme events during the growing season,

63   effects of warming winters remain understudied (Kreyling et al. 2019). In northern latitudes

64   and higher altitudes where evergreen conifers dominate, warming events are especially

65   pronounced during the winter months (IPCC 2014). In 2020, Europe experienced its warmest

66   winter on record since 1981 and the largest difference relative to the reference period (1981–

67   2020) was observed in winter over northeastern Europe (Copernicus Climate Change Service

68   2020). However, it is not clear yet how such winter warming affected winter CO_2 fluxes

69   particularly where forests are covered by snow and with high soil C content. Understanding the

70   impact of winter warming on forest net CO_2 uptake requires high temporal resolution

71   observations (sub-seasonal, daily) across many regions, as mechanisms that control forest

72   carbon fluxes are complex and show different responses to changes in climatic conditions,

73   depending on the region and forest type.

74   At the tree level, winter warming could increase CO_2 uptake in temperature-limited forests.

75   While little of this uptake is expected to be allocated to stem growth (Krejza et al. 2022), this

76   increased activity can impact physiological development of plants that are adapted to long cold

77   periods. Plant CO_2 uptake is controlled by a range of physiological responses to light,

78   temperature and CO_2 concentrations. In addition to these external drivers, physiological factors

79   (e.g., photosynthetic parameters such as light-use efficiency, maximum rate of electron

80   transport, maximum carboxylation rate, formation of carbohydrate reserves) and structural

81   characteristics (e.g., leaf area index) which vary across different evergreen needle-leaf forests

82   (ENF), directly affect how productivity and CO_2 uptake might be affected by warming in winter

83   (Martinez Vilalta et al. 2016; Stocker et al. 2018).

84   *Importance of winter period for evergreen needle-leaf forests (ENF)*

85   Forests adapted to cold environments require a persistent number of days with low temperatures

86   for building hardiness. Sudden warming during winter months can promote vegetation activity

87   in response to a condition similar to a "false spring" which can interrupt the cold hardiness

88   process (Laube et al. 2014). Additionally, increased respiration due to warming can deplete

89   stored non-structural carbohydrates (NSC) and tree hydraulic functioning (if combined with

90   drought) and affect tree functioning in spring (Sperling et al. 2015). Winter warming also affects

91   phenological development of trees and increases the chance of photo-oxidative frost damage

92   during earlier stages of the growing season (Gu et al. 2008; Chamberlain et al. 2019). All of

93   this would compromise the capacity of the forest for CO_2 uptake throughout the year (Desai et

94   al. 2016).

95   Environmental cues such as temperature, photoperiod, and light quality control a network of

96   signalling pathways that coordinate cold acclimation and cold hardiness in trees that ensure

97   survival during long periods of low temperature and freezing (Öquist and Hüner 2003;

98   Ensminger et al. 2006). These signalling pathways include the gating of cold responses by the

99   circadian clock, the interaction of light quality and photoperiod, and the involvement of

100   phytohormones in low temperature acclimation (Chang et al. 2021). Soluble carbohydrates,

101   including sucrose (most abundant) accumulate in response to low temperatures, starting from

102   late autumn throughout winter (Strimbeck & Schaberg 2009; Chang et al. 2015). Persistent

103   uninterrupted cold periods thus play an important role in forming the photosynthetic capacity

104   of the trees and their functioning under extreme climatic conditions. Experimental evidence

105   from temperature-sensitive conifers shows that warm spells in winter can induce premature

106   dehardening of buds, and result in stunted shoot development in the following spring (Nørgaard

107   Nielsen & Rasmussen, 2008). In addition to damage from frost, earlier dehardening can

108   potentially affect the capacity of trees to cope with a range of extreme climatic conditions such

109   as cold spells, drought and heat waves.

110   *Effect of warming on forest carbon fluxes*

111   Forest net ecosystem productivity (NEP) depends on the balance between gross ecosystem CO_2

112   uptake (gross primary productivity, GPP) and ecosystem respiration (Reco). Both these flux

113   components are highly sensitive to climate drivers (e.g., air and soil temperature, solar

114   radiation), and thus when canopy structural changes from one year to another are negligible,

115   the interannual variations can be predominantly explained by changes in the climatic conditions

116   (Hui et al. 2003). Net ecosystem productivity can increase or decrease with changes in air

117   temperature. In temperature-limited ecosystems for example, increase in air temperature

118   increases photosynthesis which leads to a larger gross productivity and potentially increased

119   net CO_2 uptake (if respiration does not increase more). However with warming and increased

120   temperatures, respiration (autotrophic and heterotrophic) can also increase, and the balance of

121   this with changes in gross productivity could lead to an increase, no change, or a reduction in

122   net CO_2 uptake (Gharun et al. 2020). In the presence of winter warming, despite more

123   favourable conditions for photosynthesis, factors such as water stress or photoinhibition caused

124   by high photon flux densities in combination with low air temperatures could downregulate

125   photochemical efficiency and negatively affect net photosynthesis which could decline gross

126   primary productivity (Troeng and Linder 1982).

127   The temperature sensitivity of ecosystem respiration regulates how the terrestrial CO_2

128   emissions respond to a warming climate. Within naturally occurring temperature ranges,

129   ecosystem respiration (sum of autotrophic and heterotrophic respirations) typically shows an

130   exponential increase with temperature (Lloyd and Taylor 1994). While previous studies have

131   shown an increase in Q_{10} (times of increased soil respiration with a 10 °C increase of

132   temperature) with decrease in site mean temperature (e.g., Chen et al. 2020), the temperature

133   sensitivity of ecosystem respiration incorporates both the direct response of ecosystem

134   respiration to temperature and indirect influences from other climatic and physiological

135   variables such as moisture, leaf area index, photosynthate input, litter quality, microbial

136   community (Reichstein et al. 2002; Fierer et al. 2005; Lindroth et al. 2008; Migliavacca et al.

137   2011; Karhu et al. 2014; Collalti et al. 2020). These factors change across species composition

138   and climatic regions and make predicting changes in forest carbon fluxes in response to

139   warming challenging.

140   The winter of 2019-2020 was reported as the hottest on record (1981-2022) across Europe

141   (Copernicus Climate Change Service/ECMWF). When compared to the average conditions, up

142   to 45 less winter ice days were detected in eastern Europe Russe (C3S/KNMI). In Finland, for

143   example, the average air temperature for January and February was over 6 degrees higher than

144   the 1981-2010 mean (Copernicus Climate Change Service/ECMWF). In this study we

145   investigated how the exceptionally warm winter of 2019-2020 affected ENFs in Europe. Our

146   objectives were to:

147   1) evaluate the relative change in air and soil temperature during the winter 2019-2020,

148   compared to a 6-year reference period of 2014-2019, 2) quantify the relative changes in the

149   winter CO_2 fluxes across coniferous sites with available ecosystem-level CO_2 flux

150   measurements, and 3) identify the contribution of climatic drivers (air temperature, soil

151   temperature, solar radiation) to changes in CO_2 fluxes during the warm winter. Our hypothesis

152   was that warming in winter leads to a larger negative effect on net CO_2 balance (i.e., higher

153   emissions) across colder forests. We addressed these objectives and tested our hypothesis by

154   exploring ecosystem-level CO_2 fluxes measured with eddy covariance over 98 site-years in 14

155   evergreen needle-leaf forests distributed from the Boreal to the Mediterranean regions.

156

157   **Material and Methods**

158   *Site description*

159   We selected 14 evergreen needle-leaf forests where continuous CO_2 fluxes and meteorological

160   measurements were available for at least six years until the end of 2020. Selected sites were

161   located from the northern to the southern edge of ENF forest distribution in Europe (Figure 1).

162

163   **Figure 1** Location of the 14 Evergreen Needleleaf Forest (ENF) sites included in this study.
164   Base-map is the MODIS Land Cover Product (MOD12Q1, 500m spatial resolution) showing
165   the distribution of ENFs in Europe in 2020. Elevation of the sites ranges from 4 m a.s.l. (IT-
166   SR2) to 1735 m a.s.l. (IT-Ren).
167
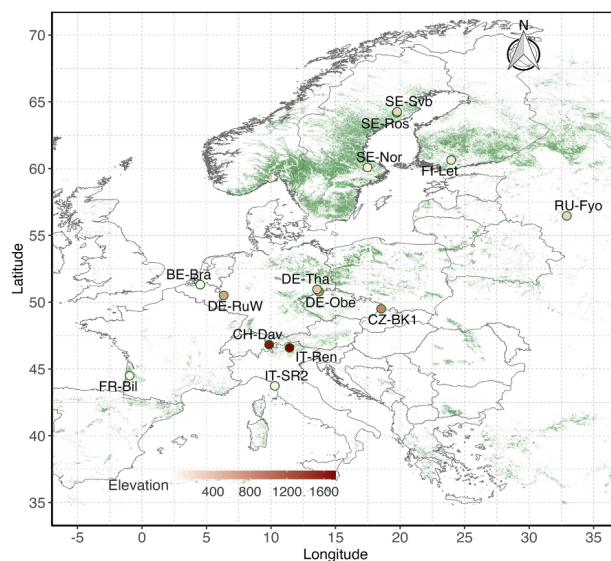
168

169 The most northern site studied is located in Sweden at 64.2 °N (SE-Svb) and the most southern

170 site in Italy at 43.7 °N (IT-SR2). Mean annual air temperature varies between 1.8 °C (in SE-Ros

171 and SE-Svb) and 15.4 °C (in IT-SR2) across sites. Mean annual total precipitation varies from 527

172 mm (in SE-Nor) to 1316 mm (in CZ-BK1). Elevation ranges from 4 m a.s.l. (IT-SR2) to 1730 m

173 a.s.l. (IT-Ren). Table 1 summarizes the description of sites including their dominant canopy

174 species.

175

176 **Table 1** Description of the 14 ENF study sites. Mean annual temperature and total precipitation
177 refer to the 2014-2019 period. Mean number of days with snow cover for each site is based on
178 the MODIS satellite observations. Sites are listed in a decreasing order in the mean annual
179 temperature.
180

Site ID	Lat. (º)	Long. (º)	Altitude (m a.s.l.)	Canopy species (dominant first)	Mean annual temperature (ºC)	Mean annual precipitation (mm)	Nr days with snow cover
IT-SR2	43.702	10.290	4	*Pinus pinea*	15.7	950	0
FR-Bil	44.493	-0.956	39	*Pinus pinaster*	14.1	930	11
BE-Bra	51.307	4.519	16	*Pinus sylvestris*	11.5	750	20
DE-Tha	50.962	13.565	385	*Picea abies*	10.2	843	41
DE-RuW	50.504	6.331	610	*Picea abies*	8.7	1250	50
DE-Obe	50.786	13.721	734	*Picea abies*	7.4	996	90
SE-Nor	60.086	17.479	45	Mixed (*Pinus sylvestris*, *Picea abies*)	7.2	527	89
CZ-Bk1	49.502	18.536	875	*Picea abies*	7.1	1316	71
RU-Fyo	56.461	32.922	265	Mixed (*Picea abies*, *Betula pubescens*)	6.1	711	58
FI-Let	60.641	23.959	111	Mixed (*Pinus sylvestris*, *Picea abies*, *Betula pubescens*)	5.9	627	99
IT-Ren	46.586	11.433	1735	*Picea abies*	5.5	809	112
CH-Dav	46.815	9.855	1639	*Picea abies*	4.8	1062	139
SE-Ros	64.172	19.738	160	*Pinus sylvestris*	4.0	614	102
SE-Svb	64.256	19.774	267	Mixed (*Pinus sylvestris*, *Picea abies*, *Betula pubescens*)	3.2	614	106

181

182 *Dataset*

183 We used the Warm Winter 2020 eddy covariance dataset processed with FLUXNET pipeline

184 (compatible with the FLUXNET2015 collection) in this study (Warm Winter 2020 Team, & ICOS

185 Ecosystem Thematic Centre, 2022); https://www.icos-cp.eu/data-products/2G60-ZHAK)

186 (Pastorello et al. 2020). We included the analysis of the spring season at each site to account for

187   the responses immediately after the winter season. Winter months included December, January,

188   and February and spring months included March, April, and May. The 6-year reference period was

189   from 2014 to 2019. This period was selected to have sufficient temporal overlap between the sites.

190   NEE quality-checked with a constant friction velocity (u*) threshold was used for all sites

191   (NEE_CUT_REF)(Shekhar et al. 2023). For an easier interpretation, we present net ecosystem

192   exchange as net ecosystem productivity (NEP = -NEE) where a negative NEP indicates that forest

193   is a net source, and positive NEP indicates forest is a net sink of CO_2 (Chapin et al. 2006).

194   In terms of climatic variables we selected those that overlapped across all sites during the study

195   period. These included incoming shortwave radiation (R_g), air temperature (T_{air}), soil temperature

196   at 5cm (T_{soil}), precipitation and top soil water content. Given that continuous long-term snow depth

197   measurements were not available at all sites, we used remotely sensed snow depth products to

198   quantify mean snow depth and snow depth anomalies in winter 2020. The snow depth data were

199   derived from the simulation of the Famine Early Warning Systems Network (FEWS NET) Land

200   Data Assimilation System (FLDAS) (McNally et al., 2017). FLDAS data are produced from the

201   Noah version 3.6.1 Land Surface Model (LSM) at a monthly resolution with a global coverage at

202   a spatial resolution of 0.1° × 0.1° (approx.10 km × 10 km) (Kumar et al., 2013) and has been used

203   in the past to study global spatiotemporal patterns of snow depth and cover (Notarnicola 2022).

204   For snow cover we used MODIS/Terra (MOD10A2) and MODIS/AQUA (MYD10A2) (Hall and

205   Riggs, 2021) Snow Cover 8-Day L3 Global 500m SIN Grid, Version 6 dataset, which provides

206   maximum snow cover extent at 8-day temporal resolution and 500m spatial resolution. For each

207   forest site, we derived average (2014-2019) leaf area index (LAI) from the LAI Collection 300 m

208   Version 1.1 product (LAI300) provided by the Copernicus Global Land Service (Fuster et al.,

209   2020). Average LAI was estimated for each site during the mean net CO_2 uptake period

210   (Supplementary Figure 2). Start of the net carbon uptake period was defined as when daily NEP

211   crosses from negative to positive, and end is the inverse.

212   *Statistical analysis*

213   We compared average daily and daytime (when $R_g > 10$ W/m^2 and local time 8-18h) means of

214   each variable (*v*; climate drivers, CO_2 fluxes) during the winter and spring of 2020 to the mean

215   from a 6-year reference period (2014-2019) using a t-test ($p < 0.05$). Daily means of each variable

216   was calculated only using the measured and good quality gap-filled half-hourly data (variable

217   quality control = 0 or 1). To understand the major drivers of winter and spring NEP for each forest

218   site, we derived conditional variable importance (CVI_v) of each predictor variable (R_g, T_{air}, and

219   T_{soil}) based on a random forest regression model (Breiman, 2001). Soil water content was removed

220   from the drivers analysis because of its negligible effect on the overall model. We tuned the

221   random forest model by iterating 'ntree' parameter (number of trees to grow) from 100 to 500 with

222   steps of 50, and 'mtry' parameter (number of variables to try at each split) from 1 to 3 with steps

223   of 1, and chose the parameter (ntree = 300 and mtry = 2) with the minimum mean square error.

224   CVI_v accounts for the correlation between the predictor variables, and was calculated using the

225   *party* R-package (Hothorn et al., 2006). Based on a 7-day moving window (centered on the central

226   value of the window) we calculated the mean daily (and daytime) NEP, T_{air}, R_g, and T_{soil}. To

227   compare the CVI_v across sites, for each site we calculated the relative CVI (RCVI) for each

228   variable as per equation 2.

229    $RCVI_v \ (\%) \ = \ \frac{CVI_v}{\sum CVI_v} \times 100$ Equation 2

230   Where $\sum CVI_v$ is the sum of CVI_v of all variables used in the model. We expressed changes in

231   variable during 2020 (v_{2020}) and the reference period ($v_{reference}$) based on its relative anomaly

232   (Δv_r) and absolute anomaly (Δv_a) as per equations 3 & 4.

233    $\Delta v_r \ (\%) \ = \ \frac{v_{2020} - v_{reference}}{|v_{reference}|} \times 100$ Equation 3

234    $\Delta v_a \ = \ v_{2020} - v_{reference}$ Equation 4

235   To further understand the how (absolute) anomalies of different variables (daytime R_g, T_{air}, T_{soil})

236   explained the variation in daytime ΔNEP, we used the RCVI (as per equation 2) derived from

237   (also) a random forest regression model with hyperparameters *ntree* = 100 and *mtry* = 3 (tuned

238   for lowest mean squared error), for each site (number of data points at least 80 days). The %

239   variance explained of the model was based on the out-of-bag estimates.

240

241   **Results**

242   *Warm winter 2019-2020 conditions across different sites*

243   According to the *in-situ* data, compared to the reference period (2014-2019), winter 2020 was the

244   warmest winter across 10 sites. In seven sites, the winter also had lower precipitation than normal

245   (Figure 2, and Supplementary Figure 1). Positive air temperature anomalies in winter 2020 were

246   larger in the high latitude or high-altitude sites compared to the mid-latitude and low-elevation

247   sites (Figure 3) with largest anomaly of 4.79 °C in RU-Fyo and lowest positive anomaly of 0.87

248   °C observed in IT-SR2 (Figure 3). The average number of snow cover days per year was highly

249   variable across the study sites. (Table 1). The southernmost site studied here (IT-SR2) typically

250   has no snow cover in winter, while the subalpine forest in Switzerland (CH-Dav) has on average

251   139 days with snow (Table 1). In those sites with consistent snow cover in winter (11 out of 14

252   sites) snow depth declined at 9 out of 11 sites during the warm winter of 2020 and reduction was

253   considerable in FI-Let, RU-Fyo, SE-Nor, DE-Obe, DE-Ruw, and DE-Tha (Figure 4). In SE-Svb,

254   FI-Let and DE-Obe soil temperature at 5 cm was continuously above the freezing level in winter

255   2020 (Figure 5), unlike the mean conditions at the sites where soil temperature fluctuates around

256   zero in winter. Changes in winter temperature were more significant in winter than in spring

257   (Figure 3), which is the reason why we focus on the effect of winter warming on CO_2 fluxes only.

258   *Effect of climate drivers on winter CO_2 fluxes*

259   The annual net productivity of ENFs varied from being a maximum sink (±sd) of 797 (± 320) g C

260   m^{-2} yr^{-1} (CZ-BK1) to a maximum source of -311 (± 93) g C m^{-2} yr^{-1} (SE-Nor) during the six-year

261   reference period (2014-2019) (Table 2). Inter-annual variation in NEP was largest in CZ-BK1 (320

262   gC m^{-2} y^{-1}) and lowest in SE-Svb (35 gC m^{-2} y^{-1}) (Table 2). The length of the net CO_2 uptake

263   period was on average 178 days but varied between the sites from 105 days (in RU-Fyo) to 315

264   days (in DE-Ruw) (Table 2, Suppl. Figure 2). Except FR-Bil and DE-RuW all sites were a CO_2

265   source in winter under reference conditions, however in IT-SR2, the forest shifted from a CO_2

266   source into a CO_2 sink in winter 2020 (Supplementary Table 1).

267   During the warm winter 2020, mean daily NEP (i.e., annual winter CO_2 sink or source strength)

268   changed significantly ($p < 0.05$) in 9 out of 14 sites (BE-Bra, CZ-BK1, DE-Obe, FI-Let, IT-Ren,

269   IT-SR2, SE-Svb, SE-Nor, RU-Fyo, grouped as the "affected" sites) compared to the 2014-2019

270   reference period, with changes in both positive and negative directions (Figure 6). For example,

271   in BE-Bra, DE-Obe, IT-Ren, SE-Svb and FI-Let, the forest became a significantly larger source

272   of CO_2 in winter 2020, while in IT-SR2, SE-Nor, CZ-BK1, and RU-Fyo forest shifted towards

273   being a smaller source for CO_2 in winter 2020 (Figure 6, Supplementary Table 1). IT-SR2 showed

274   the largest increased daily NEP in winter (346%) and BE-Bra showed the largest negative anomaly

275   in daily NEP (-97%) (Figure 6). During the warm winter ecosystem respiration (approximated by

276   nighttime NEP) increased significantly across 10 out of 14 sites (Figure 6). Daytime NEP however

277   (dominated by productivity) increased significantly with warming in only 5 sites, and mainly in

278   the warmer sites (Figure 6).

279   The relative importance results of the random forest regression analysis showed that across tested

280   variables, R_g generally had the largest control on NEP. However, with decrease in site baseline

281   (i.e., mean) temperature, the effect of R_g declined (Figure 7). For example, in the three coldest

282   sites (SE-Svb, CH-Dav, IT-Ren) R_g had a relative importance of 52%, 23% and 41% for the

283   variations in NEP respectively, while in the three warmest sites (IT-SR2, FR-Bil and BE-Bra) R_g

284   had a relative importance of 73%, 81% and 58% for NEP respectively (Figure 7). Radiation

285   dominated the effect on winter GPP and temperature dominated the effect on winter respiration

286   fluxes. Particularly in the colder sites the effect of radiation was the least (Figure 7).

287

288

289   **Figure 2** Winter temperature and precipitation anomalies (x_anom = x-x_mean) in 2020 (between
290   December 2019 and February 2020) at those sites where winter 2020 was the warmest and driest
291   relative to winters during the reference period 2014-2019. Precipitation anomalies are converted
292   to relative change (relative to mean) but temperature changes are in the original unit (°C).
293   Anomalies are classified in four main classes of "wet-warm", "dry-warm", "wet-cold", and "dry-
294   cold". Winter 2020 is marked in bold. Symbols are marked in blue and label (year) is displayed
295   only if precipitation change was larger than 10% and at the same time temperature change more
296   than 0.5 °C. Sites ordered by increasing mean temperature (SE-Svb coldest and IT-SR2 warmest).
297
298

299
300
301
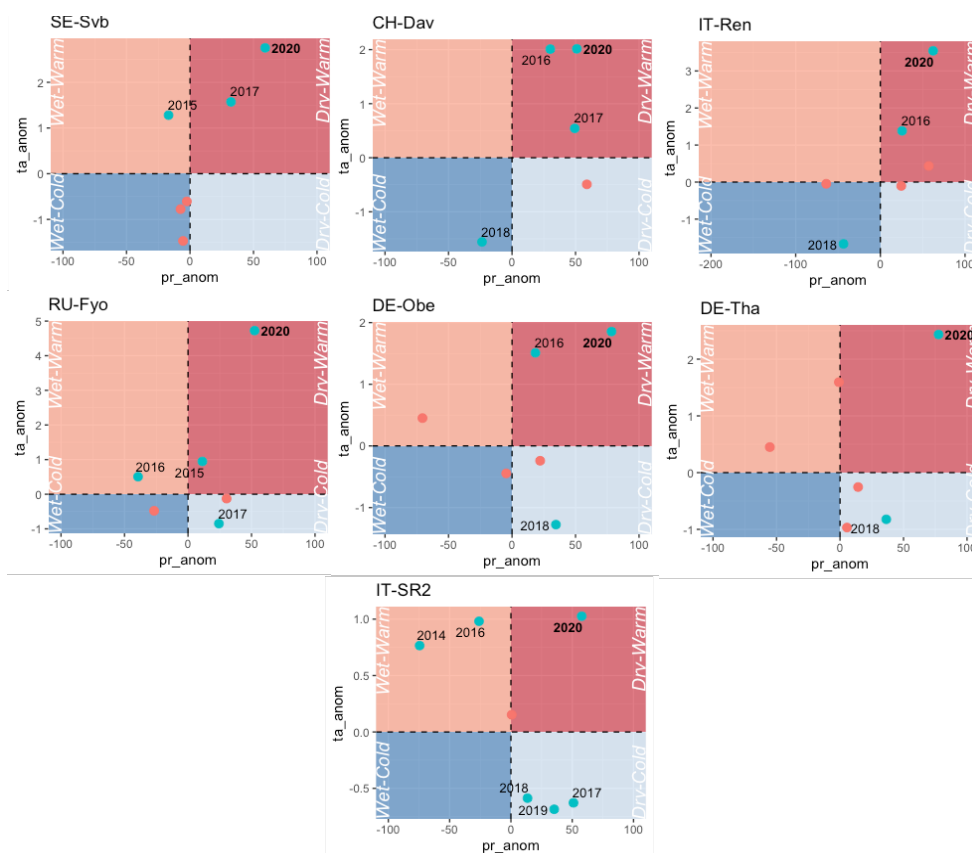
Figure 3 Seasonal changes in air temperature (T$_{air}$) and soil temperature (T$_s$) in 2020 compared to the 6-year reference period (2014-2019). Asterisk marks where means in 2020 were significantly different from the reference period (p<0.05). Anomalies were calculated from daily values. Sites are listed in a decreasing order of mean annual air temperature.
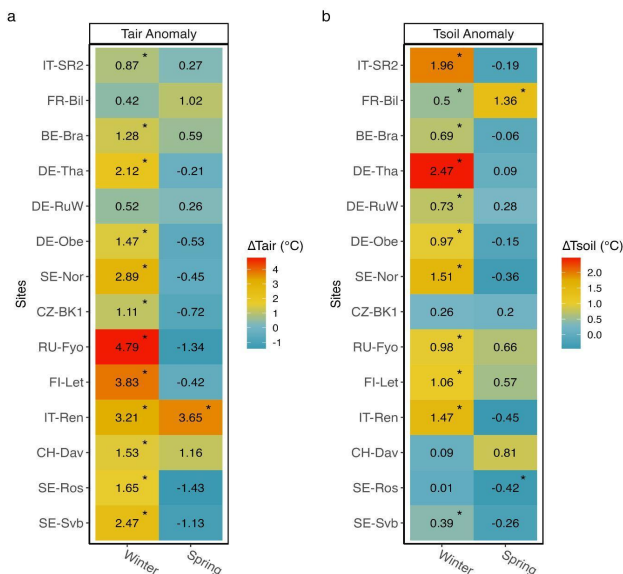
Figure 4 December to May snow depth changes (cm) in winter 2020 compared to the average winters during the reference period (2014-2019). Note that only 11 out of 14 sites have persistent snow cover in winter. Sites ordered by increasing mean temperature (SE-Svb coldest and DE-Tha warmest).
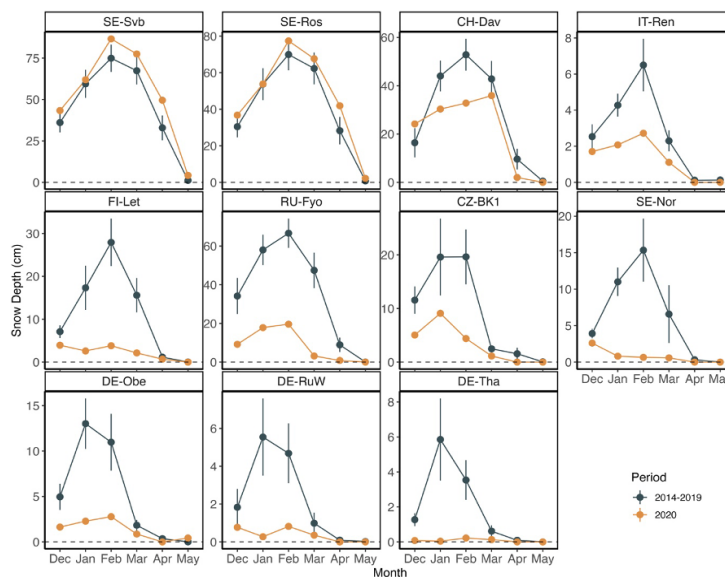
314 **Table 2** Mean total annual net ecosystem productivity (NEP) and the standard deviation (inter-
315 annual variation) during the reference period (2014 and 2019). Start of the net carbon uptake
316 period (SOS, day of year, DOY) is when daily NEP changes from negative to positive and end
317 (EOS) is the inverse (see Suppl. Figure 2). Sites are listed in a decreasing order in mean annual
318 air temperature.
319

Site ID	NEP (±sd) (g C m^{-2} y^{-1})	SOS (DOY)	EOS (DOY)	Net carbon uptake period (days)
IT-SR2	197 (±67)	35	200	165
FR-Bil	324 (±103)	20	215	195
BE-Bra	279 (±158)	95	270	175
DE-Tha	484 (±88)	55	305	250
DE-Ruw	597 (±155)	1	365	365
DE-Obe	251 (±147)	75	265	190
SE-Nor	-311 (±93)	90	200	110
CZ-Bk1	797 (±320)	70	310	240
RU-Fyo	25 (±50)	95	200	105
FI-Let	-113 (±123)	100	230	130
IT-Ren	675 (±70)	75	305	230
CH-Dav	231 (±139)	80	280	200
SE-Ros	320 (±136)	95	255	160
SE-Svb	163 (±35)	95	240	145

320
321

322 *Effect of warming on NEP anomalies*

323 Across the low latitude or low altitude (< 1000 m a.s.l.) sites where NEP changed significantly

324 in winter 2020 (IT-SR2, BE-Bra, DE-Obe), average NEP anomaly was +75%. In the high-

325 latitude-high elevation sites where NEP was significantly different in winter 2020 (SE-Nor,

326 CZ-BK1, RU-Fyo, FI-Let, IT-Ren, SE-Svb) the average NEP anomaly was -8.8% (reduced net

327 uptake) (Figure 6, Supplementary Figure 5). Average variable explained by the random forest

328 regression for daytime ΔNEP when abiotic drivers were included in winter was 72% in winter

329 (Figure 8). Across the affected sites, changes in the air temperature dominated the effect on

330 NEP anomalies (Figure 8). While FI-Let was affected by a partial cut in 2016 (Korkiakoski et

331 al. 2019; Korkiakoski et al. 2020), winter fluxes remained relatively stable in all pre- and post-

332 harvest years as the partial cut affected mostly the summer fluxes (data not shown here).

333 The relationship between air and soil temperature was stronger than radiation and air

334 temperature across sites and the relationship between air and soil temperature was stronger in

335 warmer sites (Table 3). In addition to snow cover, leaf area index and the degree of canopy

336 closure (directly related to LAI) affect the relationship between air and soil temperature through

337 a stronger shading of the soil in dense forests. CZ-BK1 had the largest LAI (4.52 ± 0.09 se)

338   and SE-Ros the smallest (2.59 ± 0.09). FI-Let had the largest inter-annual variation (± 0.27)

339   in LAI and IT-Ren and FR-Bil smallest inter-annual variation (± 0.08) (Table 3).

340

341   **Table 3** Pearson correlation coefficient between mean daily incoming shortwave
342   radiation (Rg), air temperature (T_{air}) and soil temperature at 5m (T_{soil}) at each site during
343   the reference period (2014-2019). Sites are ordered by a decreasing mean air
344   temperature. Leaf area index (LAI) values are shown as mean across the study period ±
345   standard error of the mean.

346

| Site ID	R_g-T_{air}	T_{air}-T_{soil}	LAI ± se
IT-SR2	0.69	0.97	3.12 (0.11)
FR-Bil	0.65	0.76	3.50 (0.08)
BE-Bra	0.67	0.92	4.42 (0.13)
DE-Tha	0.73	0.96	4.04 (0.19)
DE-RuW	0.59	0.83	2.99 (0.22)
DE-Obe	0.72	0.94	3.69 (0.21)
SE-Nor	0.71	0.90	3.08 (0.09)
CZ-Bk1	0.72	0.92	4.52 (0.09)
RU-Fyo	0.74	0.78	4.06 (0.14)
FI-Let	0.66	0.88	3.29 (0.27)
IT-Ren	0.64	0.84	3.54 (0.08)
CH-Dav	0.63	0.87	3.25 (0.12)
SE-Ros	0.69	0.77	2.59 (0.09)
SE-Svb	0.71	0.84	2.79 (0.12)

347
348
349
350   **Figure 5** Soil temperature (at 5cm) changes in winter 2020 compared to the reference period
351   (2014-2019). Shaded bands around the mean show the 95% confidence interval of mean soil
352   temperature. Sites are ordered (top and right to left) by increasing baseline temperature (SE-
353   Svb coldest and IT-SR2 warmest).
354
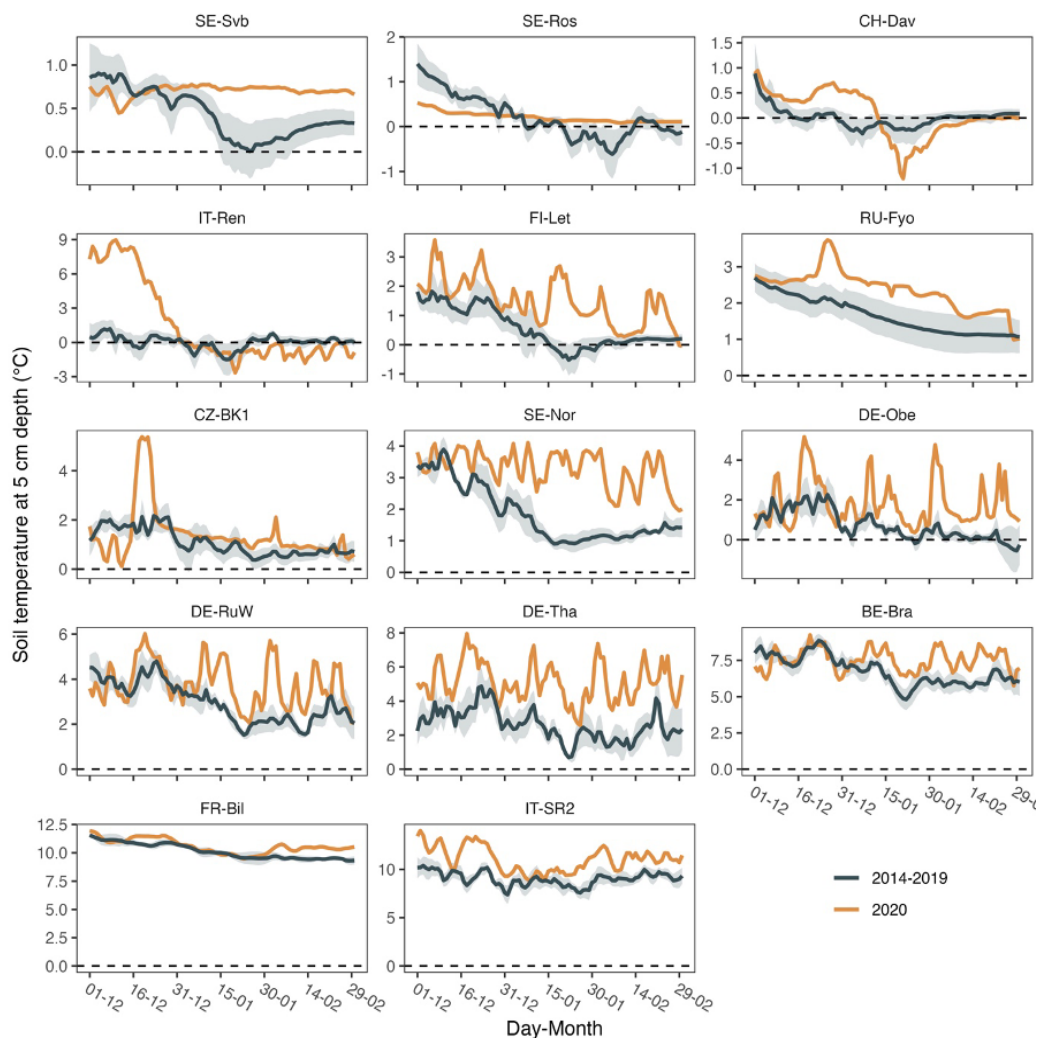
Figure 6 Relative changes (%) in mean daily, nighttime, and daytime NEP in winter 2020 compared to the 6-year reference winters (2014-2019). Asterisks mark where means in 2020 were significantly different from the reference period ($p < 0.05$). Positive NEP change indicates increased net uptake (due to increased uptake or reduced emission) and negative change indicates decreased net uptake (due to reduced uptake or increased emission). Sites are listed in a decreasing mean annual air temperature order.
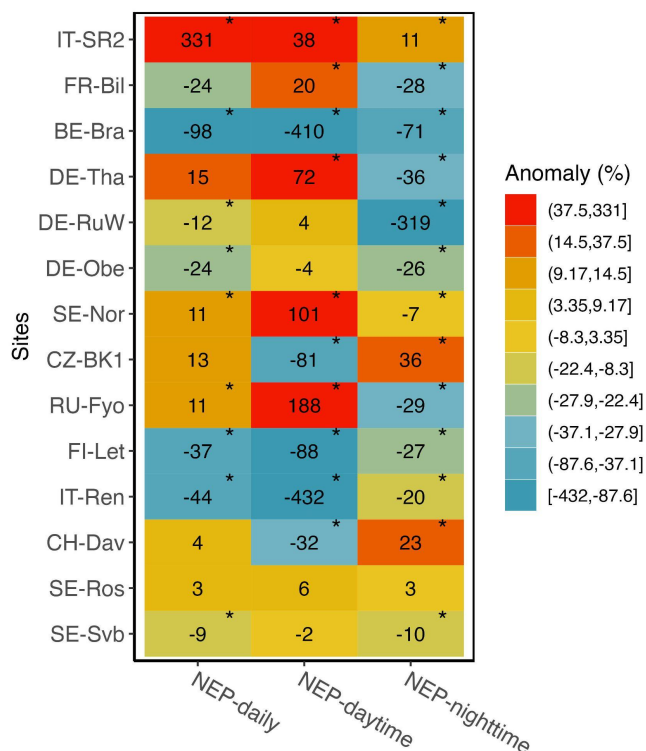
394 **Figure 7** Relative conditional variable importance (RCVI, %) of three climatic variables for
395 daily winter NEP, GPP and Reco, and the overall variable explained (marked with red
396 triangles) estimated from the random forest regression analysis. The RFR model was trained
397 on winter observations during the reference period (2014-2019). The sites are ordered by
398 decreasing mean annual temperature (top to bottom).
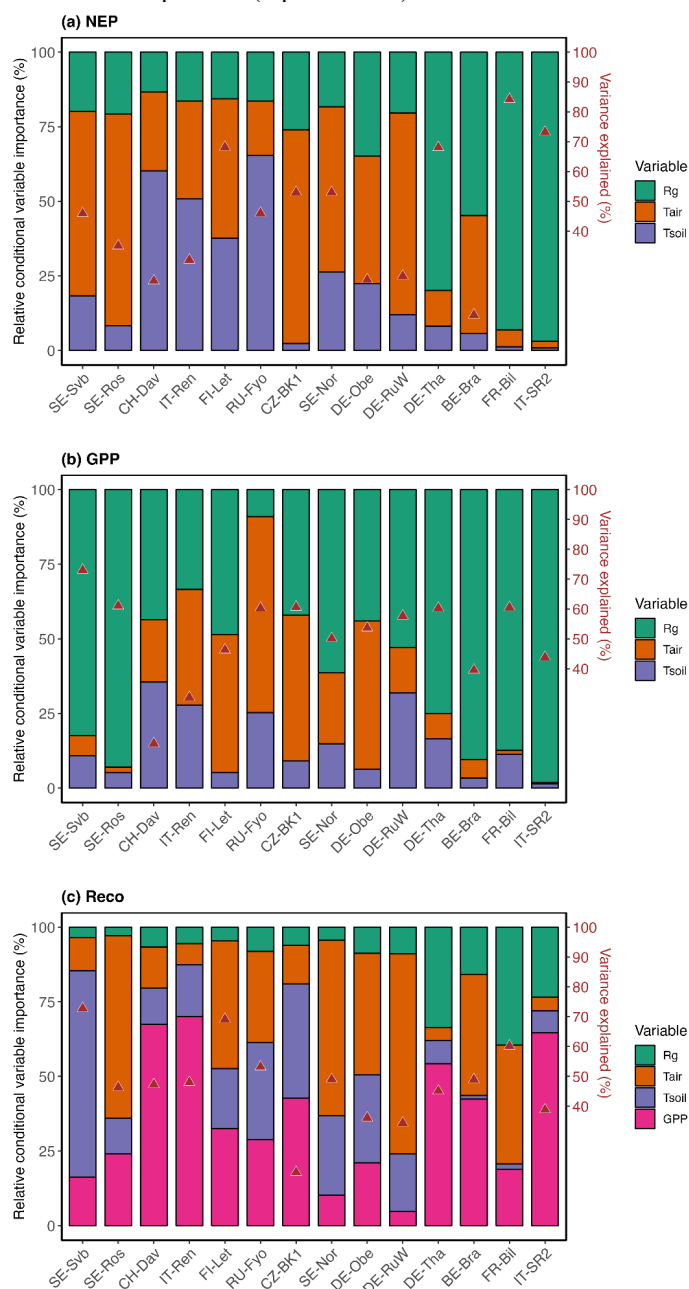
399
400

401   **Figure 8** Comparison of the relative importance of abiotic (T_{air}, R_g, T_s) variables, for NEP
402   changes (ΔNEP) in winter 2020. R^2 of the RFR model that was used to explain the variation
403   in daytime ΔNEP (i.e., when PPFD > 0) is shown on the secondary (right) y-axis and marked
404   with red triangles. Sites are ordered by increasing mean air temperature (from left to right).
405

Relative conditional variable importance for Winter daytime ΔNEP
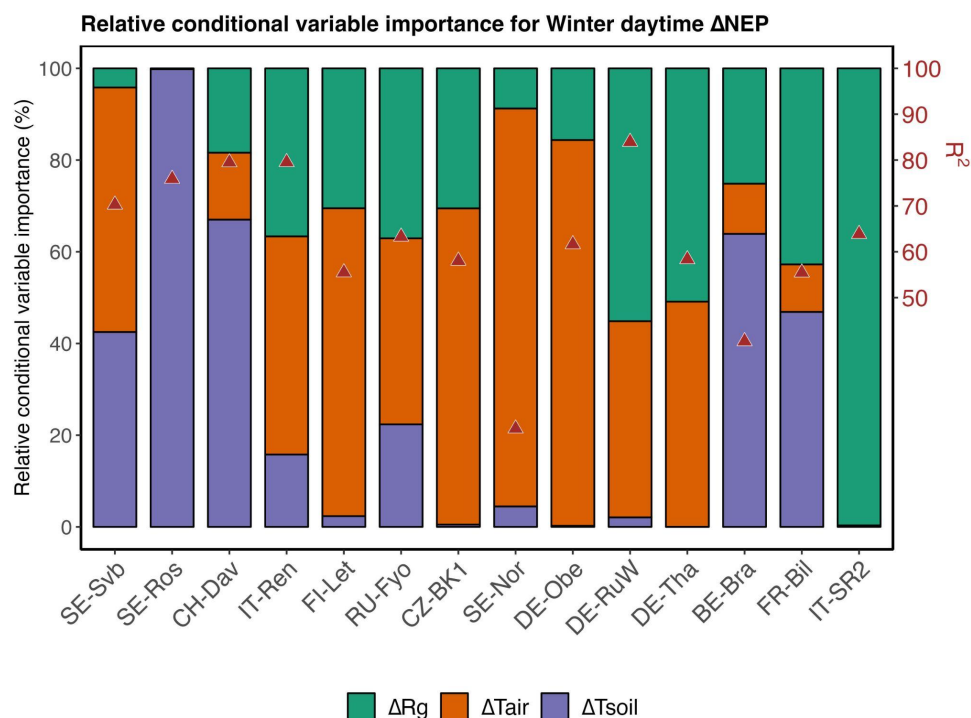
406
407
408
409   **Discussion**

410   *Warming of the air and the soil in winter*

411   We tested how climate variables and CO_2 fluxes deviated from a reference period (2014-2019)

412   during the warm winter of 2020 , across 14 evergreen needle-leaf forest sites distributed from

413   north to south of Europe (from Sweden to Italy). The sites where winter 2020 was particularly

414   warm and dry were not clustered in a certain climatic region, however we observed a consistent

415   pattern that warming of the air was more pronounced in the northern latitude and on high

416   altitudes sites, while in lower latitudes and altitudes warming of the soil was more pronounced

417   (Figure 3). While in forests top soil temperature is directly affected by changes in the air

418   temperature, several underlying processes and properties modify the magnitude of decoupling

419   of air and soil temperature which could reach up to 10 degrees, depending on the season and

420   properties of the biome type (Lembrechts et al. 2022). These underlying factors and processes

421   include for example 1) a vertically complex and horizontally continuous forest structure that

422   leads to higher decoupling of the soil temperature from air temperature, 2) soil moisture content

423   as moisture increases the soil heat storage, 3) insulation by the litter or snow cover, 4) cloud

424   cover, ground surface albedo, and rate of evapotranspiration which collectively affect the

425   radiation balance and energy exchange between the soil and the air, and 5) microtopography

426   that affects the drainage of air (e.g., cool air drains in low-lying areas) (Guan et al., 2009;

427   Lozano-Parra et al., 2018; De Frenne et al., 2021; Gril et al., 2023). Given that in our study the

428   type of forest was similar across sites (all sites were dominated by evergreen needle-leaf

429   forests) and given that our focus was on the warming during the winter season, we attribute the

430   main source of difference in the soil and air temperature to two main factors. First the snow

431   depth that ranged from no snow to over 100 cm across sites (Table 1, Figure 4), and second,

432   differences in forest structure (e.g, LAI) which varied between 2.59 to 4.52 across the sites

433   (Table 3). We observed that the sites with the smaller snow depth showed a larger warming of

434   the soil during the warm winter of 2020 perhaps because the insulating effect of snow cover

435   was weaker here (Friesen et al. 2021) (Figure 2, Figure 4). At the sites where snow depth

436   declined significantly in winter 2020, soil temperatures increased substantially with large

437   fluctuations over the season, whereas in other sites with greater snow depth such soil

438   temperature fluctuations were absent (Figure 5). The link between warming of the air and

439   warming of the soil was also controlled by the canopy structure as we found a significant

440   positive relationship between the two ($p < 0.05$, $r = 0.69$). Although the direct effect of canopy

441   closure on snow distribution, accumulation and melting at different periods was not tested here,

442   it was evident that sites that had a larger LAI also showed a tighter coupling between air

443   temperature and soil temperature as forest canopy closure reduces snow depth (Table 3)(Woods

444   et al. 2006; Gao et al. 2022).

445   *Winter warming effect on forest CO_2 fluxes*

446   Our general observation was that across sites with a lower mean average temperature (i.e., high

447   altitude or high latitude sites) winter warming was concurrent with increased net CO_2

448   emissions. In the warmer sites however (low altitude or low latitude sites) winter warming also

449   increased the productivity and CO_2 uptake (Supplementary Figure 5). This difference can

450   generally be explained by the balance of changes in the warming of the soil versus warming of

451   the air (Bond-Lamberty and Thomson 2010) which affects both soil respiration and tree CO_2

452   uptake. Where soil becomes proportionally warmer and soil temperature reaches above

453   freezing levels, root activity is enhanced and tree productivity responds directly to the increased

454   air temperatures, and CO_2 uptake increases. Warming of the air - if not translated into a direct

455   warming of the soil– might not enhance productivity if the soil within the rooting zone remains

456   frozen. In IT-Ren for example where daytime NEP declined significantly in the warm winter,

457   air temperature increased to over 3.5 degrees more than normal, however soil temperature

458   remained at freezing levels (Figure 5).

459   CO_2 fluxes are sensitive to changes in both temperature and light (e.g., incoming radiation) and

460   site baseline climate conditions showed to be a good proxy of how changes in light and air

461   temperature lead to changes in NEP (Figure 7). There is however evidence that temperature

462   responses of biochemical processes are a function of plant growth temperature, and not just

463   instantaneous temperature (Fürstenau Togashi et al. 2018). In addition, response of NEP to

464   similar temperature can be different across seasons (i.e., an evident hysteresis), depending on

465   other environmental factors such as solar radiation and soil water content (Niu et al. 2011).

466   While across different sites sensitivity of NEP to temperature increases with a decrease in site

467   mean temperature, as site mean temperature increases (temperature is no longer limiting)

468   radiation becomes a larger constraint on NEP (Running et al. 2004).

469   Chamber-based observations from boreal forests show that snow-depth and soil moisture affect

470   temperature sensitivity of soil CO_2 fluxes as the freeze-thaw cycles abruptly change the

471   moisture content of the soil (Du et al., 2013). In that sense, warmer winters can trigger larger

472   respiration (and availability of nutrients to trees) because of higher Q_{10} of thawed than frozen

473   soils (Wang et al., 2014), however microbial C limitation can reduce expected increase in

474   respired CO_2, if not countered by greater labile C inputs (Sullivan et al., 2020). In addition,

475   aboveground productivity increases with increase in temperature (Supplementary Figure 3) and

476   enhances the autotrophic respiration. Warming in winter also affects the microbial community

477   that control labile and stable organic carbon decomposition in the soil that would offset

478   respiration response to temperature and lead to a reduction of soil respiration under warming

479   (Tian et al., 2021). The magnitude of increase in belowground autotrophic respiration in

480   response to warming and the supply of labile substrate through rhizodeposition and root

481   exudate also affects net CO_2 fluxes under warming (Nyberg et al., 2020). Decrease in the snow

482   pack and increased soil freezing has short-term immediate impacts on plant CO_2 uptake, but

483   can also leave a long-lasting negative impact on functioning of trees (Repo et al. 2021).

484   Particularly sites with prolonged cold winter seasons could be rather negatively affected by the

485   warming in winter, as we observed through reduced daytime NEP which is an indication of

486   stress from warming during winter. Trees growing in northern latitudes and higher altitudes

487   could be more negatively affected by warming in winter as optimal temperatures in trees are

488   regulated by the short-term changes in temperature, whereas in ecosystems where temperature

489   fluctuations are seasonally larger, optimal temperature for growth has a broader range (Weng

490   et al. 2010; Liu 2020).

491

492   *Winter tree physiology effect on CO_2 fluxes*

493   Responses of coniferous species to soil warming can vary largely depending on the species'

494   adaptive traits, the overall ecosystem context, and interactions with other environmental factors

495   such as precipitation, temperature, and nutrient availability (Dawes et al. 2017; Oddi et al.

496   2022). The sites we studied here, although all were dominated by evergreen needle-leaf species,

497   consisted of different canopy species and some sites were dominated by a mixture of species

498   (Table 1). There can be significant differences in photosynthetic parameters across different

499   species of evergreen conifers that would affect tree and ecosystem response to warming

500   (Fürstenau Togashi et al. 2018). The different responses of productivity to increased warming

501   in ENFs can stem from differences in the quantity (and quality) of stored NSC in the roots, and

502   the rate at which this C storage is mobilized within the tree during the warm winter (Bansal

503   and Germino 2009). Warmer temperatures and dry conditions in winter lead to stomatal closure

504   and depletion of carbohydrate reserves for trees that are adapted to ample precipitation and low

505   VPD conditions in winter, and this effect leads to reduced CO_2 uptake of trees during warmer

506   winters (Earles et al. 2018).

507   Low temperature is essential for signals that trigger the synthesis of soluble carbohydrates

508   involved in osmotic and freezing protection against cold extremes (Chang et al. 2021) that

509   otherwise impair the Calvin cycle by inhibiting the regeneration of ribulose bisphosphate

510   (RuBP) and decrease the efficiency of Rubisco carboxylation (Ensminger et al. 2012; Crosatti

511   et al. 2013). Non-structural carbohydrates (sugar and starch) that are accumulated during the

512   growing season are utilized in winter to ensure survival of trees (Zhu et al. 2012; Tixier et al.

513   2020) and failure to develop overwintering defences can cause evergreen conifer needles to

514   remain susceptible for example to photo-oxidative damage during frost events (Chang et al.

515   2016).

516   Our results provide the first analysis of the effect of winter warming on CO_2 fluxes of evergreen

517   needle-leaf forests in Europe and point to the importance of understanding multiple underlying

518   mechanisms that govern CO_2 fluxes. Data on the responses of photosynthetic traits on a

519   timescale that is ecologically relevant (days to years) are scarce, but eddy covariance

520   observations provide an opportunity for constructing long-term time series of canopy level

521 processes to investigate the effect of extreme climatic conditions across all seasons. We

522 encourage studies that combine long-term observations and plant-level experiments to

523 investigate how changes in the functioning in winter might affect trees' response to extremes

524 that occur earlier in the growing season (e.g., spring frost, spring drought) and to understand

525 the consequences of such extremes for ecosystem carbon uptake.

526

527 **Conclusion**

528 Our study investigated the effect of winter warming on CO_2 fluxes of evergreen needle-leaf

529 forests across Europe during the warm 2019-2020 winter. We found significant differences in

530 the impact of warming across sites, with northern and higher-altitude locations experiencing

531 more significant warming of the air, while southern and lower-altitude sites saw greater soil

532 warming. Winter warming influenced forest CO_2 fluxes, with daytime Net Ecosystem

533 Productivity (NEP) decreasing in colder sites due to lower soil temperature, while warmer sites

534 experienced increased CO_2 uptake. However, responses were not similar across all sites, and

535 factors such as forest structure, and local mean climatic conditions played a role in creating

536 microclimates that buffer or enhance the impact of warming on CO_2 fluxes. Understanding

537 these variations combined with tree ecophysiological functioning of cold-adapte ecosystems is

538 crucial for predicting how forests will respond to future winter warming.

539

550

551 *Data availability:* The dataset used in this study is openly available from the ICOS

552 Carbon Portal. https://doi.org/10.18160/2G60-ZHAK

553

554 *Author contributions:* MG designed the study; MG and AS performed the data analysis;

555 MG wrote the manuscript, and all authors commented on the analysis and contributed

556 substantially to the writing of the manuscript.

557

558 *Competing interests:* The authors declare that they have no conflict of interests.

559 **References**

560 Bansal S, Germino MJ (2009) Temporal variation of nonstructural carbohydrates in montane
561   conifers: similarities and differences among developmental stages, species and
562   environmental conditions. Tree Physiology 9(4), 559-568, DOI:
563   10.1093/treephys/tpn045

564 Bond-Lamberty, B., Thomson, A. Temperature-associated increases in the global soil
565   respiration record. Nature 464, 579–582 (2010). https://doi.org/10.1038/nature08930

566 Breiman, L. (2001). Random forests. Machine Learning, 45(1), 5–32.
567   https://doi.org/10.1023/A:1010933404324

568 Chamberlain, C. J., Cook, B. I., García de Cortázar-Atauri, I., & Wolkovich, E. M. (2019).
569   Rethinking false spring risk. Global Change Biology, 25(7), 2209-2220.
570   doi:https://doi.org/10.1111/gcb.14642

571 Chang, C. Y., Unda, F., Zubilewich, A., Mansfield, S. D., & Ensminger, I. (2015). Sensitivity
572   of cold acclimation to elevated autumn temperature in field-grown Pinus strobus
573   seedlings. Frontiers in Plant Science, 6.

574 Chang, C. Y., Fréchette, E., Unda, F., Mansfield, S. D., & Ensminger, I. (2016). Elevated
575   temperature and CO2 stimulate late-season photosynthesis but impair cold hardening in
576   pine. plant physiology, 172(2), 802-818.
577   doi:10.1104/pp.16.00753doi:10.3389/fpls.2015.00165

578 Chang, C. Y.-Y., Bräutigam, K., Hüner, N. P. A., & Ensminger, I. (2021). Champions of
579   winter survival: cold acclimation and molecular regulation of cold hardiness in
580   evergreen conifers. New Phytologist, 229(2), 675-691.
581   doi:https://doi.org/10.1111/nph.16904

582 Chapin, F.S., Woodwell, G.M., Randerson, J.T. et al. Reconciling Carbon-cycle Concepts,
583   Terminology, and Methods. Ecosystems 9, 1041–1050 (2006).
584   https://doi.org/10.1007/s10021-005-0105-7

585 Chen, JL., Reynolds, J.F., Harley, P.C. et al. (1993) Coordination theory of leaf nitrogen
586   distribution in a canopy. Oecologia 93, 63–69. https://doi.org/10.1007/BF00321192

587 Chen S, Wang J, Zhang T, Hu Z (2020) Climatic, soil, and vegetation controls of the
588   temperature sensitivity (Q10) of soil respiration across terrestrial biomes. Global
589   Ecology and Conservation 22, e00955

590 Collalti, A. et al. Plant respiration: controlled by photosynthesis or biomass? Glob. Change
591   Biol. 26, 1739–1753 (2020).

592 Crosatti, C., Rizza, F., Badeck, F.-W., Mazzucotelli, E., & Cattivelli, L. (2013). Harden the
593   chloroplast to protect the plant. Physiologia Plantarum, 147 1, 55-63.

594 Dawes, M.A., Schleppi, P., Hättenschwiler, S., Rixen, C. and Hagedorn, F. (2017), Soil
595   warming opens the nitrogen cycle at the alpine treeline. Glob Change Biol, 23: 421-434.
596   https://doi.org/10.1111/gcb.13365

597 De Frenne, P., Lenoir, J., Luoto, M., Scheffers, B.R., Zellweger, F., Aalto, J., Ashcroft, M.B.,
598   Christiansen, D.M., Decocq, G., De Pauw, K., Govaert, S., Greiser, C., Gril, E., Hampe,
599   A., Jucker, T., Klinges, D.H., Koelemeijer, I.A., Lembrechts, J.J., Marrec, R., Meeussen,
600   C., Ogée, J., Tyystjärvi, V., Vangansbeke, P. and Hylander, K. (2021), Forest
601   microclimates and climate change: Importance, drivers and future research agenda. Glob

602   Change Biol, 27: 2279-2297. https://doi.org/10.1111/gcb.15569

603 Desai A., G. Wohlfahrt, M.J. Zeeman, G. Katata, W. Eugster, L. Montagnani, D. Gianelle, M.
604   Mauder and H-P Schmid (2016) Montane ecosystem productivity responds more to
605   global circulation patterns than climatic trends. Environmental Research Letters, 11,
606   024013.

607 Du E. et al., (2013) Winter soil respiration during soil-freezing process in a boreal forest in
608   Northeast China, Journal of Plant Ecology, Volume 6, Issue 5, Pages 349–357,
609   https://doi.org/10.1093/jpe/rtt012

610 Earles, J.M., Stevens, J.T., Sperling, O., Orozco, J., North, M.P. and Zwieniecki, M.A.
611   (2018), Extreme mid-winter drought weakens tree hydraulic–carbohydrate systems and
612   slows growth. New Phytol, 219: 89-97. https://doi.org/10.1111/nph.15136

613 Ensminger, I., Busch, F., & Huner, N. P. A. (2006). Photostasis and cold acclimation: sensing
614   low temperature through photosynthesis. Physiologia Plantarum, 126(1), 28-44.
615   doi:https://doi.org/10.1111/j.1399-3054.2006.00627.x

616 Ensminger, I., Berninger, F., & Streb, P. (2012). Response of photosynthesis to low
617   temperature. In J. Flexas, F. Loreto, & H. Medrano (Eds.), Terrestrial photosynthesis in
618   a changing environment: a molecular, physiological, and ecological approach (pp. 276–
619   293): UK: Cambridge University Press.

620 Fierer, N., Craine, J. M., McLauchlan, K. & Schimel, J. P. Litter quality and the temperature
621   sensitivity of decomposition. Ecology 86, 320–326 (2005).

622 Friedlingstein, P., O'Sullivan, M., Jones, M. W., Andrew, R. M., Bakker, D. C. E., Hauck, J.,
623   Landschützer, P., Le Quéré, C., Luijkx, I. T., Peters, G. P., Peters, W., Pongratz, J.,
624   Schwingshackl, C., Sitch, S., Canadell, J. G., Ciais, P., Jackson, R. B., Alin, S. R.,
625   Anthoni, P., Barbero, L., Bates, N. R., Becker, M., Bellouin, N., Decharme, B., Bopp,
626   L., Brasika, I. B. M., Cadule, P., Chamberlain, M. A., Chandra, N., Chau, T.-T.-T.,
627   Chevallier, F., Chini, L. P., Cronin, M., Dou, X., Enyo, K., Evans, W., Falk, S., Feely,
628   R. A., Feng, L., Ford, D. J., Gasser, T., Ghattas, J., Gkritzalis, T., Grassi, G., Gregor, L.,
629   Gruber, N., Gürses, Ö., Harris, I., Hefner, M., Heinke, J., Houghton, R. A., Hurtt, G. C.,
630   Iida, Y., Ilyina, T., Jacobson, A. R., Jain, A., Jarníková, T., Jersild, A., Jiang, F., Jin, Z.,
631   Joos, F., Kato, E., Keeling, R. F., Kennedy, D., Klein Goldewijk, K., Knauer, J.,
632   Korsbakken, J. I., Körtzinger, A., Lan, X., Lefèvre, N., Li, H., Liu, J., Liu, Z., Ma, L.,
633   Marland, G., Mayot, N., McGuire, P. C., McKinley, G. A., Meyer, G., Morgan, E. J.,
634   Munro, D. R., Nakaoka, S.-I., Niwa, Y., O'Brien, K. M., Olsen, A., Omar, A. M., Ono,
635   T., Paulsen, M., Pierrot, D., Pocock, K., Poulter, B., Powis, C. M., Rehder, G.,
636   Resplandy, L., Robertson, E., Rödenbeck, C., Rosan, T. M., Schwinger, J., Séférian, R.,
637   Smallman, T. L., Smith, S. M., Sospedra-Alfonso, R., Sun, Q., Sutton, A. J., Sweeney,
638   C., Takao, S., Tans, P. P., Tian, H., Tilbrook, B., Tsujino, H., Tubiello, F., van der Werf,
639   G. R., van Ooijen, E., Wanninkhof, R., Watanabe, M., Wimart-Rousseau, C., Yang, D.,
640   Yang, X., Yuan, W., Yue, X., Zaehle, S., Zeng, J., and Zheng, B.: Global Carbon Budget
641   2023, Earth Syst. Sci. Data, 15, 5301–5369, https://doi.org/10.5194/essd-15-5301-2023,
642   2023.

643 Friesen, H.C., Slesak, R.A., Karwan, D.L., Kolka, R.K., (2021) Effects of snow and climate
644   on soil temperature and frost development in forested peatlands in Minnesota, USA.
645   Geoderma 394, 115015.

646 Foyer, C.H., Neukermans, J., Queval, G., Noctor, G., Harbinson, J. (2012) Photosynthetic

647 control of electron transport and the regulation of gene expression. J. Exp. Bot., 63, pp.
648   1637-1661

649 Fürstenau Togashi, H., Prentice, I. C., Atkin, O. K., Macfarlane, C., Prober, S. M.,
650   Bloomfield, K. J., and Evans, B. J. (2018) Thermal acclimation of leaf photosynthetic
651   traits in an evergreen woodland, consistent with the coordination hypothesis,
652   Biogeosciences, 15, 3461–3474, https://doi.org/10.5194/bg-15-3461-2018.

653 Fuster, B., Sánchez-Zapero, J., Camacho, F., García-Santos, V., Verger, A., Lacaze, R.,
654   Weiss, M., Baret, F., & Smets, B. (2020). Quality assessment of PROBA-V LAI,
655   fAPAR and fCOVER collection 300 m products of Copernicus global land service.
656   Remote Sensing, 12(6), 1017. https://doi.org/10.3390/rs1206101

657 Gao, Y., Shen, L., Cai, R., Wang, A., Yuan, F., Wu, J., Guan, D., & Yao, H. (2022). Impact
658   of Forest Canopy Closure on Snow Processes in the Changbai Mountains, Northeast
659   China. Frontiers in Environmental Science, 10, Article 929309.
660   https://doi.org/10.3389/fenvs.2022.929309

661 Gharun, M., Hörtnagl, L., Paul-Limoges, E., Ghiasi, S., Feigenwinter, I., Burri, S.,
662   Marquardt, K., Etzold, S., Zweifel, R., Eugster, W., & Buchmann, N. (2020).
663   Physiological response of Swiss ecosystems to 2018 drought across plant types and
664   elevation. Philosophical Transactions of the Royal Society B: Biological Sciences,
665   375(1810), 20190521. https://doi.org/10.1098/rstb.2019.0521

666 Gril, E., Spicher, F., Greiser, C., Ashcroft, M. B., Pincebourde, S., Durrieu, S., Nicolas, M.,
667   Richard, B., Decocq, G., Marrec, R., & Lenoir, J. (2023). Slope and equilibrium: A
668   parsimonious and flexible approach to model microclimate. Methods in Ecology and
669   Evolution, 14, 885– 897. https://doi.org/10.1111/2041-210X.14048

670 Gu L, et al. (2008) The 2007 Eastern US Spring Freeze: Increased Cold Damage in a
671   Warming World?, *BioScience*, Volume 58, Issue 3, March 2008, Pages 253–
672   262, https://doi.org/10.1641/B580311

673 Guan, X., Huang, J., Guo, N. et al. (2009) Variability of soil moisture and its relationship
674   with surface albedo and soil thermal parameters over the Loess Plateau. Adv. Atmos.
675   Sci. 26, 692–700. https://doi.org/10.1007/s00376-009-8198-0

676 Hall, D. K. and G. A. Riggs. MODIS/Terra Snow Cover 8-Day L3 Global 500m SIN Grid,
677   Version 6. 2021, Distributed by NASA National Snow and Ice Data Center Distributed
678   Active Archive Center.

679 Hothorn, T., Hornik, K., and Zeileis, A.: Unbiased Recursive Partitioning: A Conditional
680   Inference Framework, J. Comput. Graph. Stat., 15, 651–674,
681   https://doi.org/10.1198/106186006X133933, 2006.

682 Hui, D., Luo, Y., & Katul, G. (2003). Partitioning interannual variability in net ecosystem
683   exchange between climatic variability and functional change. Tree Physiology, 23(7),
684   433-442. doi:10.1093/treephys/23.7.433

685 IPCC, 2014: Climate Change 2014: Synthesis Report. Contribution of Working Groups I, II
686   and III to the Fifth Assessment Report of the Intergovernmental Panel on Climate
687   Change [Core Writing Team, R.K. Pachauri and L.A. Meyer (eds.)]. IPCC, Geneva,
688   Switzerland, 151 pp.

689 Karhu, K., Auffret, M., Dungait, J. et al. Temperature sensitivity of soil respiration rates
690   enhanced by microbial community response. Nature 513, 81–84 (2014).
691   https://doi.org/10.1038/nature13604

692 Knauer, J., El-Madany, T. S., Zaehle, S., & Migliavacca, M. (2018). Bigleaf-An R package
693   for the calculation of physical and physiological ecosystem properties from eddy
694   covariance data. PLoS ONE, 13(8), e0201114. doi:10.1371/journal.pone.0201114

695 Korkiakoski M, Tuovinen JP, Penttilä T, Sarkkola S, Ojanen P, Minkkinen K, Rainne J,
696   Laurila T, Lohila A (2019) Greenhouse gas and energy fluxes in a boreal peatland forest
697   after clear-cutting, Biogeosciences 16, pp. 3703-3723, 10.5194/bg-16-3703-2019

698 Korkiakoski M, Ojanen P, Penttilä I, Minkkinen K, Sarkkola S, Rainne J, Laurila T, Lohila A
699   (2020) Impact of partial harvest on CH4 and N2O balances of a drained boreal peatland
700   forest, Agricultural and Forest Meteorology 295, 108168,
701   https://doi.org/10.1016/j.agrformet.2020.108168

702 Krejza, J., Haeni, M., Darenova, E., Foltýnová, L., Fajstavr, M., Světlík, J., … Zweifel, R.
703   (2022). Disentangling carbon uptake and allocation in the stems of a spruce forest.
704   Environmental and Experimental Botany, 196, 104787,
705   https://doi.org/10.1016/j.envexpbot.2022.104787

706 Kreyling, J., Grant, K., Hammerl, V. et al. (2019) Winter warming is ecologically more
707   relevant than summer warming in a cool-temperate grassland. Sci Rep 9, 14632.
708   https://doi.org/10.1038/s41598-019-51221-w

709 Kumar, S. V. et al. (2013) Multiscale evaluation of the improvements in surface snow
710   simulation through terrain adjustments to radiation. J. Hydrometeorol. 14, 220–232.

711 Lasslop,G.,Reichstein,M.,Papale,D.,Richardson,A.,Arneth,A., Barr, A., Stoy, P., and
712   Wohlfahrt, G. (2010) Separation of net ecosystem exchange into assimilation and
713   respiration using a light response curve approach: critical issues and global evaluation,
714   Glob. Change Biol., 16, 187–208, https://doi.org/10.1111/j.13652486.2009.02041.x

715 Laube, J. et al., Chilling outweighs photoperiod in preventing precocious spring development.
716   Glob. Change Biol. 20, 170–182 (2014).

717 Lembrechts, J. J., van den Hoogen, J., Aalto, J., Ashcroft, M. B., De Frenne, P., Kemppinen,
718   J., Kopecký, M., Luoto, M., Maclean, I. M. D., Crowther, T. W., Bailey, J. J., Haesen, S.,
719   Klinges, D. H., Niittynen, P., Scheffers, B. R., Van Meerbeek, K., Aartsma, P.,
720   Abdalaze, O., Abedi, M., … Lenoir, J. (2022). Global maps of soil temperature. Global
721   Change Biology, 28, 3110– 3144. https://doi.org/10.1111/gcb.16060

722 Lindroth, A. et al. Leaf area index is the principal scaling parameter for both gross
723   photosynthesis and ecosystem respiration of Northern deciduous and coniferous forests.
724   Tellus B 60, 129–142 (2008).

725 Liu Y. (2020) Optimum temperature for photosynthesis: from leaf- to ecosystem-scale. Sci
726   Bull 65(8):601-604. doi: 10.1016/j.scib.2020.01.006.

727 Lloyd J, Taylor JA (1994) On the temperature dependence of soil respiration. Funct. Ecol., 8
728   (1994), pp. 315-323

729 Lozano-Parra J, Pulido M, Lozano-Fondón C, Schnabel S. (2018) How do Soil Moisture and
730   Vegetation Covers Influence Soil Temperature in Drylands of Mediterranean Regions?
731   Water 10(12):1747. https://doi.org/10.3390/w10121747

732 Maire V, Martre P, Kattge J, Gastal F, Esser G, Fontaine S, et al. (2012) The Coordination of
733   Leaf Photosynthesis Links C and N Fluxes in C3 Plant Species. PLoS ONE 7(6): e38345.
734   https://doi.org/10.1371/journal.pone.0038345

735 Martinez Vilalta, J., Sala, A., Asensio, D., Galiano, L., Hoch, Gü., Palacio, S., Piper, F.,
736   Lloret, F.. (2016). Dynamics of non-structural carbohydrates in terrestrial plants: A
737   global synthesis. Ecological Monographs. 86. 10.1002/ecm.1231.

738 McNally, A. et al. (2017) A land data assimilation system for sub-Saharan Africa food and
739   water security applications. Sci. Data 4, 170012. https://doi.org/10.1038/sdata.2017.12

740 Migliavacca, M. et al. Semiempirical modeling of abiotic and biotic factors controlling
741   ecosystem respiration across eddy covariance sites. Glob. Change Biol. 17, 390–409
742   (2011).
743   Niu S., Luo Y., Fei S., Montagnani L., Bohrer G., Janssens I.A., Gielen B., Rambal S.,
744   Moors E., Matteucci G., (2011). Seasonal hysteresis of net ecosystem exchange in
745   response to temperature change: patterns and causes. Global Change Biology, 17, 3102-
746   3114, DOI: 10.1111/j.1365-2486.2011.02459.x.

747 Nørgaard Nielsen, C. C., & Rasmussen, H. N. (2008). Frost hardening and dehardening in
748   Abies procera and other conifers under differing temperature regimes and warm-spell
749   treatments. Forestry: An International Journal of Forest Research, 82(1), 43-59.
750   doi:10.1093/forestry/cpn048

751 Notarnicola, C. Overall negative trends for snow cover extent and duration in global
752   mountain regions over 1982–2020. Sci Rep 12, 13731 (2022).
753   https://doi.org/10.1038/s41598-022-16743-w.

754 Nyberg, M. and Hovenden, M. J. (2020) Warming increases soil respiration in a carbon-rich
755   soil without changing microbial respiratory potential, Biogeosciences, 17, 4405–4420,
756   https://doi.org/10.5194/bg-17-4405-2020.

757 Öquist, G., & Huner, N. P. A. (2003). Photosynthesis of Overwintering Evergreen Plants.
758   Annual Review of Plant Biology, 54(1), 329-355.
759   doi:10.1146/annurev.arplant.54.072402.115741

760 Oddi et al (2022) Contrasting responses of forest growth and carbon sequestration to heat and
761   drought in the Alps, Environ. Res. Lett. 17, 045015, doi:10.1088/1748-9326/ac5b3a

762 Pastorello, G., Trotta, C., Canfora, E. et al. The FLUXNET2015 dataset and the ONEFlux
763   processing pipeline for eddy covariance data. Sci Data 7, 225 (2020).
764   https://doi.org/10.1038/s41597-020-0534-3

765 Reichstein, M. et al. Ecosystem respiration in two Mediterranean evergreen holm oak forests:
766   drought effects and decomposition dynamics. Funct. Ecol. 16, 27–39 (2002).
767 Repo, T., Domisch, T., Kilpeläinen, J. et al. Soil frost affects stem diameter growth of
768   Norway spruce with delay. Trees 35, 761–767 (2021). https://doi.org/10.1007/s00468-
769   020-02074-8

Running SW, Nemani RR, Heinsch FA, Zhao M, Reeves M, Hashimoto H (2004). A
    Continuous Satellite-Derived Measure of Global Terrestrial Primary Production,
    BioScience, Volume 54, Issue 6, Pages 547–560, https://doi.org/10.1641/0006-
    3568(2004)054[0547:ACSMOG]2.0.CO;2

Shekhar, A., Hörtnagl, L., Buchmann, N., & Gharun, M. (2023). Long-term changes in forest
    response to extreme atmospheric dryness. Global Change Biology, 00, 1– 18.
    https://doi.org/10.1111/gcb.16846

Sperling, O., Earles, J.M., Secchi, F., Godfrey, J., Zwieniecki, M.A. (2015) Frost induces
    respiration and accelerates carbon depletion in trees. PLoS ONE 10(2): e0144124. doi:
    10.1371/journal.pone.0144124

Stocker, B.D., Zscheischler, J., Keenan, T.F., Prentice, I.C., Peñuelas, J. and Seneviratne, S.I.
    (2018), Quantifying soil moisture impacts on light use efficiency across biomes. New
    Phytol, 218: 1430-1449. https://doi.org/10.1111/nph.15123

Strimbeck, G. R., & Schaberg, P. G. (2009). Going to extremes: low temperature tolerance
    and acclimation in temperate and boreal conifers. In M. T. Gusta L.; Wisniewski, K.,
    (Ed.), Plant cold hardiness: from the laboratory to the field (pp. 226-239): Wallingford,
    Oxfordshire, UK: CABI Publishing.

Sullivan, P.F., Stokes, M.C., McMillan, C.K. et al. (2020) Labile carbon limits late winter
    microbial activity near Arctic treeline. Nat Commun 11, 4024.
    https://doi.org/10.1038/s41467-020-17790-5

Tian, J., Zong, N., Hartley, I.P., He, N., Zhang, J., Powlson, D., Zhou, J., Kuzyakov, Y.,
    Zhang, F., Yu, G. and Dungait, J.A.J. (2021), Microbial metabolic response to winter
    warming stabilizes soil carbon. Glob Change Biol, 27: 2011-2028.
    https://doi.org/10.1111/gcb.15538

Tixier, A., Guzmán-Delgado, P., Sperling, O. et al. Comparison of phenological traits, growth
    patterns, and seasonal dynamics of non-structural carbohydrate in Mediterranean tree
    crop species. Sci Rep 10, 347 (2020). https://doi.org/10.1038/s41598-019-57016-3

Troeng E, Linder S (1982) Gas exchange in a 20-year-old stand of Scots pine .1. Net
    photosynthesis of current and one-year-old shoots within and between seasons, Physiol.
    Plant. 54: 15-23.

Walker et al. (2014) The relationship of leaf photosynthetic traits – Vcmax and Jmax – to leaf
    nitrogen, leaf phosphorus, and specific leaf area: a meta-analysis and modeling study.
    Ecology and Evolution 2014 4(16): 3218– 3235

Warm Winter 2020 Team, & ICOS Ecosystem Thematic Centre. (2022). Warm Winter 2020
    ecosystem eddy covariance flux product for 73 stations in FLUXNET-Archive format—
    release 2022-1 (Version 1.0). ICOS Carbon Portal. https://doi.org/10.18160/2G60-
    ZHAK

Wang, Y., et al. (2014), Non-growing-season soil respiration is controlled by freezing and
    thawing processes in the summer monsoon-dominated Tibetan alpine grassland, Global
    Biogeochem. Cycles, 28, 1081– 1095, doi:10.1002/2013GB004760.

Weng, Jen-Hsien & Liao, T.-S. (2010). Photosynthetic responses and acclimation to
    temperature in seven conifers grown from low to high elevations in subtropical Taiwan.
    Taiwan Journal of Forest Science. 25. 117-127.

813   Woods, S. W., Ahl, R., Sappington, J., and McCaughey, W. (2006). Snow Accumulation in
814   Thinned Lodgepole Pine Stands, Montana, USA. For. Ecol. Manag. 235 (1-3), 202–211.
815   doi:10.1016/j.foreco.2006.08.013

816   Wullschleger, S.D. (1993) Biochemical limitations to carbon assimilation in C3 plants - a
817   retrospective analysis of the A/Ci curves from 109 species. J. Exp. Bot., 44, pp. 907-920

818   Zhu WZ, Xiang JS, Wang SG, Li MH (2012) Resprouting ability and mobile carbohydrate
819   reserves in an oak shrubland decline with increasing elevation on the eastern edge of the
820   Qinghai-Tibet Plateau. For Ecol Manage 278:118–1